

# Formulation and Evaluation of Transdermal Dissolved Microneedles Patches for Meloxicam

Laila A. Alwan,<sup>1</sup> Entidhar J. Al-Akkam<sup>2\*</sup>

<sup>1</sup>Diyala Health Department, Ministry of Health, Baghdad, Iraq

<sup>2</sup>Department of Pharmaceutics, College of Pharmacy, University of Baghdad, Baghdad, Iraq

Received: 28th May, 2021; Revised: 28th June, 2021; Accepted: 27th August, 2021; Available Online: 25th September, 2021

## ABSTRACT

Meloxicam (MLX) is a nonsteroidal anti-inflammatory medicine (NSAID) that is used to treat rheumatoid arthritis, osteoarthritis, and other joint conditions. Despite MLX's low toxicity, oral administration is linked to adverse gastrointestinal effects such as perforation and ulceration. As a result, an alternative mode of administration for MLX is required to minimize the drawbacks associated with currently available oral medicines. Drug delivery through the skin could be a suitable option since it allows medications to be delivered directly to the illness site, resulting in maximum local effects with minimal systemic activity. Molding is the most common process for making MLX polymer microneedle (MN) patches. After adding the MLX to the surfactant, different types of polymer (polyvinyl pyrrolidone (PVPK30), polyvinyl alcohol (PVA), sodium alginate (SA), and hydroxymethyl cellulose (HPMC) with different ratios and by using DW as a solvent. Afterward, the effect of type and the ratio of polymer used was studied to make the formulation better. Patches were investigated for needle morphology, drug content, axial fracture force measurement, and drug release, with the optimized formulae also being tested for pH, folding endurance, and ex vivo permeation. The PVA patch with 17.5% solid content, 10% PEG 400, and 0.25 percent glycerin has an axial needle fracture force of 30 N/100MN, which is sufficient for skin penetration. The release was quick, with about all of the medication being released in just 60 minutes. With a steady-state flux of around 3.1 times that of the ordinary patch, permeation was greatly improved. In comparison to a regular patch, MN has a lower lag time. According to the findings, the MLX MN patch could improve medication permeability while allowing for quick and painless administration.

**Keywords:** Dermal delivery, Hydroxypropyl methylcellulose (HPMC), Microneedle, Meloxicam, Polyvinyl pyrrolidone (PVPK30), Polyvinyl alcohol, Sodium alginate.

International Journal of Drug Delivery Technology (2021); DOI: 10.25258/ijddt.11.3.2

**How to cite this article:** Alwan LA, Al-Akkam EJ. Formulation and Evaluation of Transdermal Dissolved Microneedles Patches for Meloxicam. International Journal of Drug Delivery Technology. 2021;11(3):656-662.

**Source of support:** Nil.

**Conflict of interest:** None

## INTRODUCTION

Skin is a multilayered organ that protects the body from the environment by acting as a permeation barrier for exogenous molecules. The epidermis;<sup>1</sup> nonviable epidermis<sup>2-4</sup> and viable epidermis,<sup>5</sup> dermis, and hypodermis<sup>3</sup> are the three primary layers of the skin.<sup>6</sup> The stratum corneum (SC), the skin's uppermost layer, is where the skin's barrier properties are found.<sup>7,8</sup> Since this nonviable layer is thought to be the rate-limiting step for skin absorption of most molecules; percutaneous permeation is thought to be regulated by Fick's laws of diffusion.

The Microneedles (MNs) were first introduced in 1976, and an American patent for the MN for transdermal delivery was issued at the same time.<sup>9</sup> MN applications in biomedicine were initially focused on drug delivery. In the fields of medicine and pharmacy, drug delivery of pharmacologically active ingredients is critical. Oral administration,<sup>10</sup> parenteral administration,<sup>11</sup> transdermal

delivery,<sup>12</sup> and other penetration-enhancing methods are some of the ways active pharmaceutical compositions of drugs can be administered. Since MNs only penetrate the robust stratum corneum and viable epidermis, nerve endings, and blood vessels are not reached, the patient will not experience pain during the procedure.<sup>13</sup>

They are different types of MNs<sup>14</sup>; Solid MNs can be used as skin pretreatment to create large pores for drug delivery<sup>15</sup>. Coated MNs with a coating serves two purposes. The first is to pierce the skin, and the second is to add desired drugs to the surface of the MN,<sup>16</sup> negatively charged deoxyribonucleic acid (DNA) or virus was easily absorbed on positively charged MN using electrostatic attraction to achieve MN coating.<sup>17</sup> They are dissolving MNs without residual fragments<sup>18</sup> hollow MNs for liquid formulations<sup>19</sup> and hydrogel-forming.<sup>20</sup>

Meloxicam (MLX) it is a member of the oxicam chemical family. Because of its analgesic, antipyretic, and anti-inflammatory properties are used to treat rheumatoid arthritis

\*Author for Correspondence: laylaalakawy@gmail.com.

(RA), osteoarthritis (OA), and juvenile rheumatoid arthritis.<sup>21</sup> It's accessible in both oral and parenteral dose forms on the market. The oral dose of MLX ranges from 7.5 to 15 mg, and while it is generally well taken, it does induce some adverse effects, the most common of which are gastrointestinal.<sup>22</sup>

The goal of this research is to develop a dissolvable MN patch for MLX that has higher penetration bypassing the SC and analyze the various materials needed to optimize the formula.

## MATERIALS

Hyper-Chem LTD CO (China) provided MLX, Sigma-Aldrich (Germany) provided Polyvinylpyrrolidone K30 (PVP K30), Central Drug House (P) Ltd (India) provided water-soluble PVA, HiMedia laboratories in India provided Sodium alginate(SA), and Provizer Pharma, in India provided HydroxypropylmethylcelluloseE5 (HPMC E5). Polyethylene glycol PEG 400 from Riedel-De-Han, (Germany), Na<sub>2</sub>HPO<sub>4</sub> from Thomas Baker(India), Potassium dihydrogen phosphate (KH<sub>2</sub>PO<sub>4</sub>) Merck, (Germany), and Blue Silica gel powder from Om Chemicals (India).

## METHODS

### Preparation of Meloxicam Microneedles (MN) Patches

Micro molding techniques were used to make MLX MN patches, as shown in Table 1. Heating different types and ratio made a polymer solution after the MLX is added to a surfactant with 20 ml of DW for 20 minutes on a magnetic stirrer at 60°C.

The prepared polymer gel solution was transferred into micro molds which sonicated for 1.5 hours to ensure even and consistent distribution while also removing air spaces—after the process was completed, allowed to dry for 2 days in vacuum dissector and then in the oven at 40°C for 24 hours to ensure drying and needle formation before being placed in the freezer for 30 minutes at 4°C to facilitate the separation of the MN patch from the micro molds.

### Meloxicam Conventional Patch Preparation

Ordinary patches were created by utilizing the same solution mixture of MLX and polymers in specific proportions as in preparation MLX MN, but instead of utilizing the PMDS

MN mold, the mixture was cast in a petri dish. The patch was chopped into smaller patches with the same surface as MN patches that resulted from a mold after it had dried completely.

## Characterization and Evaluation of MNs Patches

### Formulation

#### Visual Review

Prepared patches of the MN were visually monitored for flaws. Only needles and patches with no abnormalities were analyzed further.

#### Dimensional Analysis

To analyze the needle geometry and quantify the tip radius, length, and height of the MN, many approaches are used. Optical or electrical microscopy are the most frequent methods. A 3D image analysis provides a clearer understanding of needle shape and aids in quality control. This was accomplished using a scanning electron microscope (SEM).<sup>23,24</sup>

#### Mechanical Properties

The elasticity of MN patches is measured by folding endurance. MN patch FE was determined by repeatedly collapsing a narrow strip of MN patches at the same spot until it was broken. The value of folding endurance is determined by the number of times the stripe is broken during collapsible.<sup>25,26</sup>

A TA-XT2i texture analyzer (Stable Micro Systems, Haslemere, UK) was used to test the mechanical properties of the MNs in compression mode, as described in a previous study (Pamornpathomkul *et al.* 2018). The test distance was set to 900 μm meters, and the trigger type was set to auto. The test speed was 0.1 mm/s, while the pre-and post-test speeds were 1 mm/s. 0.02 N was chosen as the trigger force. The tips of the MNs were maintained up by an axial compression force applied by the texture analyzer. As the needles began to break, the force was analyzed to create a force-displacement curve, and the failure force of MNs was recorded. Finally, a microscope was used to examine the compressed MNs' morphology.<sup>26</sup>

#### In-vitro Drug release Studies

The drug release was assessed using a dissolution device and a modified franz cell. MN patches were placed on a wire mesh with an 800-micrometer sieve opening and attached with an elastic band

**Table 1:** MNs patches formulas prepared by molding method

| Formulas | PVPK30 (gm) | PVA (gm) | HPMC E5 (gm) | Sodium alginate (SA) (gm) | DW (mL) | Glyn (mL) | PEG 400 (mL) |
|----------|-------------|----------|--------------|---------------------------|---------|-----------|--------------|
| F1       | 4           |          |              |                           | 20      | 0.5       | 2            |
| F2       |             | 4        |              |                           | 20      | 0.5       | 2            |
| F3       |             |          | 4            |                           | 20      | 0.5       | 2            |
| F4       |             |          |              | 4                         | 20      | 0.5       | 2            |
| F5       | 3.5         |          |              |                           | 20      | 0.5       | 2            |
| F6       |             | 3.5      |              |                           | 20      | 0.5       | 2            |
| F7       |             |          | 3.5          |                           | 20      | 0.5       | 2            |
| F8       |             |          |              | 3.5                       | 20      | 0.5       | 2            |
| F9       | 3           |          |              |                           | 20      | 0.5       | 2            |
| F10      |             | 3        |              |                           | 20      | 0.5       | 2            |
| F11      |             |          | 3            |                           | 20      | 0.5       | 2            |
| F12      |             |          |              | 3                         | 20      | 0.5       | 2            |

Oring on the open end of the tube in which the patch is placed in the center.<sup>27,28</sup> The tube was immersed in a dissolution equipment beaker containing 500 mL of phosphate buffer (pH 7.4), which was sufficient to ensure sink condition based on the drug loading. The speed of the apparatus was adjusted to 50 rpm,<sup>29</sup> and the temperature was kept at 35°C.<sup>30</sup> The experiment lasted an hour, with samples taken every 5 minutes. A 5 mL sample was removed from the beaker and replaced with 5 mL of fresh buffer. Finally, the cumulative drug release percent was determined using the MLX calibration curve in 7.4 pH phosphate buffer.

#### Drug content

Formulas had their drug content confirmed by immersing one patch in phosphate buffer pH 7.4 until completely dissolved. After that, 1 mL of this solution was transferred to a 30 mL volumetric flask, and the final volume was calculated using the same solutions. After filtration, the produced solution's absorbance was measured using an MLX max UV visible spectrophotometer. The percentage of drug content was calculated, and the procedure was repeated three times.<sup>31</sup>

#### pH Measurement on the Surface

Because an acidic or basic pH might irritate the skin membrane, determining the surface pH is critical for determining the possibility of any side effects when employing the MN *in vivo*. A 2 mL of distilled water was poured on the surface of MN patches and allowed to swell for 1-hour before the pH of the patches was tested using pH-paper.<sup>32,33</sup>

#### Variation in Weight

A weight variation test confirms the regularity of the MN patches generated. Each batch's ten randomly selected patches are individually weighed and compared to the mean weight for deviation.<sup>34</sup>

#### Measurement of Thickness

The average thickness of MN patches was assessed by employing a digital vernier caliper at five separate locations (the center and four corners). This is required to ensure that the thickness of the film is uniform, as it is directly related to the dosing precision in each patch.<sup>35</sup>

#### Percent of Moisture Loss (PML)

The purpose of this research was to see how drying conditions affected the MN patches. The PML was evaluated by drying three MN patches from each batch in a desiccator for three days using anhydrous calcium chloride at 25°C. The MN patches were weighed before being placed in the desiccator, yielding (W<sub>0</sub>), then reweighed after three days to yield (W<sub>t</sub>), and the PML was calculated using the following equation:

$$PML = \frac{W_0 - W_t}{W_0} \times 100\%$$

Where; W<sub>0</sub> = initial weight, W<sub>t</sub> = final weight<sup>36,37</sup>

#### Percentage of Water Absorbed (PMA)

The purpose of this test was to see how dampness affected the MN patches. Three MN patches from each batch were placed in a desiccator for three days in a wet setting (75% relative

humidity using a saturated potassium sulfate solution) at 25°C temperature. The MN patches were carefully weighed before being placed in the desiccator, yielding (W<sub>0</sub>), and then reweighed after three days to yield (W<sub>t</sub>) and The PMA was calculated using the following formula:

$$PMA = \frac{W_0 - W_t}{W_0} \times 100\%$$

Where; W<sub>0</sub>= initial weight, W<sub>t</sub> = final weight<sup>38,37</sup>

#### Ex-vivo penetration of MLX

For the *ex-vivo* permeation examination of the MN patches, the abdomen skin of mature male wistar rats weighing 250 ± 10g. The stratum corneum towards the upper side of the inverted glass tube in beaker (modified Franz diffusion cell), as shown in Figure 1 with a diffusion area of 1.77 cm<sup>2</sup> was used to assess *ex-vivo* drug penetration. Thumb force was used to insert the dissolving MNs array into the skin, which was subsequently fixed between the donor and acceptor compartments of the modified Franz diffusion cell at intervals of 1-hour from 1-8 hours. And at 12 hours, aliquots of 2 mL sample were removed from the receptor compartment and replaced with the same volume of receptor fluid as soon as feasible. The samples were spectrophotometrically examined for drug concentration at a wavelength of 362 nm. Each trial was carried out three times.<sup>39</sup>

## RESULTS AND DISCUSSION

#### Visual Appearance

All of the successful patches had obvious MNs and a defined yellow with no medication precipitation after ocular inspection. MN patches were made in twelve formulas (F1–F12). Because of faults in elasticity, strength, and needle formation, some formulas (F1, F3, F4, F7, F8, F11, and F12) were omitted from the study. The failure of (F1, F4, F8, and F12) was caused by the excessive viscosity of the polymer matrix, which made vacuum application difficult to fill the MN cavities of the mold.

#### Dimensional of MNs

As described in formulations, compositions were prepared. The current study results displayed that all MN patches prepared with PVA or PVP-K30 showed homogenous polymer mixtures with



Figure 1: Modified Franz diffusion cell

the resulting MNs having sharp needle tips. The form showed to be more effective in penetration and cutaneous delivery. The needles were arranged in a 12\*12 array in an 8\*8 mm patch with a 500  $\mu\text{m}$  center-to-center interval. As shown in Figure 2 show different picture of the selected formula F6.

### Mechanical Properties of MNs Patches

Folding test initially was done for measuring the elasticity of the selected formulas as shown in Table 2.

Results revealed that formulas F5 and F9 had less optimal elasticity than formulas (F2, F5, F6, and F10) they were broken that due to the present of PVPK30 in these formulas due to defects in elasticity, weakness and needles formation, which complies with research done on this polymer for elasticity and rigidity (Figure 2).<sup>40</sup> It has been shown that the PVP percentage of dissolving MNs lower can penetrate the skin due to lack in strength.<sup>41</sup>

The needles must be capable of puncturing the skin.<sup>42,43</sup> In this experiment, the mechanical strength was determined in vitro using a texture analyzer. The pressure force grew gradually with increasing displacement at first, then rapidly when the displacement exceeded 0.2 mm. When the displacement exceeded 0.80 mm, the force reduced dramatically.

In this experiment, F2, F6, and 10 of the dissolving MNs resulted in a failure force of 30, 25, and 23 N/100MN, respectively, demonstrating that MNs were strong enough to pierce skin while the other formulas will be a failure, as shown in Table 3, due to PVA is a water-soluble synthetic polymer that keeps the viscosity of the preparation at the level needed to improve patch mechanical strength.<sup>40</sup> The fracture force test revealed that the higher the PVA concentration, the harder and more rigid the patch created; hence, as the PVA concentration

rises, the applied force (N) required to break the patch rises, which is consistent with earlier research on this polymer.<sup>28</sup>

In F5 and F9 The results showed that when the ratio of PVP-K30 in the polymeric solution blend rose, the needle fraction force decreased,<sup>44,45</sup> Table 3 shows the results.

### In-vitro Drug Release Studies

Drug release was carried out under sink conditions at pH 7.4 in this experiment. Because of PVA and PVP- K30's water solubility, there was an initial burst of drug release after 10 minutes, with a cumulative released proportion of up to 90%, as seen in Figure 3. After then, the release rate reduced; after 20 minutes, roughly 100 percent of MLX was released into the receiver medium, and the cumulative amount remained nearly unchanged from 20 minutes to 1-hour.

Formulas with effective MN formation were used to investigate the influence of the type of polymer used (PVP, PVA) drug release. The release of (F2, F5, F6, F9, and F10) in 60 minutes was 100%, classifying them as fast-release formulations. In addition, the cumulative MLX release was almost equivalent to the drug content in MNs, which presumably means that the matrix materials had no interference in drug release from MNs. It has been demonstrated that the present of PVP in dissolving MNs reduces the time required for dissolution and generates holes in the MNs with water, resulting in an increased dissolution rate. However, the higher the amount of PVP, the lower the ability to penetrate the skin due to a lack of strength.<sup>41</sup> Both hygroscopicity and moisture adsorption properties of PVP are linked to its effects, which resulted in hydration and the burst effect, which made drug release from patches containing higher amounts of PVP faster.<sup>46</sup>

To increase medication release, PEG400 was added in F2, F5, F6, F9, and F10. The improvement induced by PEG400

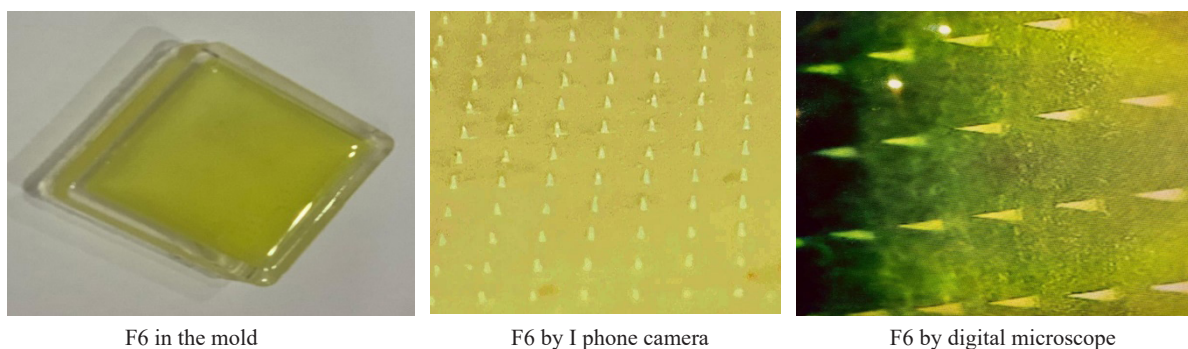


Figure 2: different pictures of selected formula F6.

Table 2: Folding endurance for MNs patches formulas

| Formula number | Folding Endurance |
|----------------|-------------------|
| F2             | 132               |
| F5             | 38                |
| F6             | 122               |
| F9             | 50                |
| F10            | 98                |

Table 3: Needle fraction force (N) per 100 MN for MNs patches formulas. mean  $\pm$  SD) n=3

| Formula number | Needle fraction force (N) per 100 MN* |
|----------------|---------------------------------------|
| F2             | 30 $\pm$ 0.235                        |
| F5             | 18 $\pm$ 35                           |
| F6             | 25.67 $\pm$ 0.422                     |
| F9             | 22.80 $\pm$ 0.236                     |
| F10            | 23.10 $\pm$ 0.364                     |

was attributable to a decrease in interfacial tension, which increased the wetting of the polymer to a greater extent, resulting in increased polymer erosion.<sup>47</sup>

### Drug Content

The results showed that F2,F5,F6,F9,F10,F11and F12 the formulation was suitable and that the content was uniform. The drug content was in range of (97–99%) According to USP38/NF33 (2015), the percent label amount can range from 85.0 to 115.0% and the percent standard deviation (percent SD) of the dose entity shall not exceed 6% (Table 4)<sup>48</sup>

### pH on the surface of MNs

All of the successfully constructed MN patches had appropriate surface pH values ranging from 6.3 to 6.6 (Table 5), and when compared to the pH of the skin (5.5), the resultant MN patches did not induce skin irritation.

### Variation in Weight and Thickness

The average weights for the created formulations ranged from 447.2 to 463 mg (Table 6), suggesting that the MN patch preparation approach is repeatable and produces patches of consistent weight. The patch weights were calculated using digital balancing, and all patches are consistent.

Table 6 shows the average thickness values of the created MN patches.<sup>49</sup> The values were found to range from 0.52 to 0.56 millimeters. A low standard deviation figure indicates that the approach used to prepare MN patches was repeatable, resulting in patches of a consistent thickness and, as a result, dose precision in each patch may be assured.

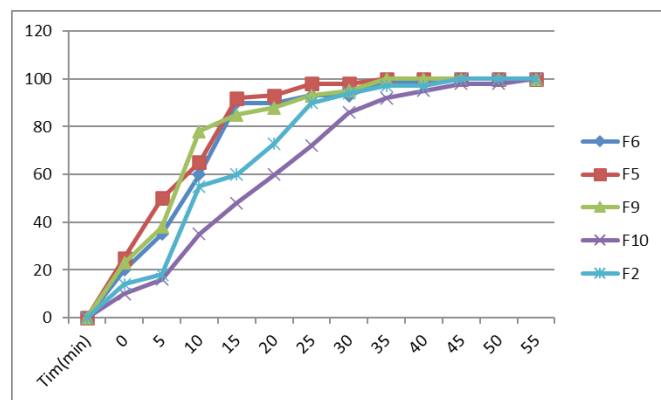


Figure 3: The drug release from selected formulas

Table 4: The Drug Content Percent of MN Patches (mean  $\pm$  SD) n = 3

| Formula number | Drug content %    |
|----------------|-------------------|
| F2             | 97.47 $\pm$ 0.101 |
| F5             | 98.25 $\pm$ 0.211 |
| F6             | 97.77 $\pm$ 0.221 |
| F9             | 98.17 $\pm$ 0.221 |
| F10            | 98.12 $\pm$ 0.233 |
| F11            | 97.33 $\pm$ 0.172 |
| F12            | 99.51 $\pm$ 0.038 |

### Percent of Moisture Loss (PML)

The moisture loss study provides insight into the nature, stability, and ability of MNs patches to maintain their physicochemical qualities under normal storage settings. It also provides information on the hydrophilicity of MN patches. Table 7 contains all of the acquired results. The obtained results are nearly homogeneous, ranging from 2.12 to 3.54 percent, indicating minimal moisture loss and stable formulations.

### Percentage of Water Absorbed (PMA)

The presence of moisture bearings is a vital examination on drug stability. Thus a moisture uptake study is an important aspect to be evaluated. Table 7 lists all of the moisture uptake values was reported. All of the polymers were found to be hydrophilic in nature, with moisture absorption values ranging from 6.43 to 12.57%.

### Ex-vivo Penetration of MLX

Full-thickness isolated rat skin was used in this experiment as a drug permeable membrane. The ordinary MLX patch that was applied to the intact skin showed inferior permeability. Figure 4

Table 5: The PH on the surface of MN patches (mean  $\pm$  SD) n = 3

| Formula number | pH on the surface |
|----------------|-------------------|
| F2             | 6.3 $\pm$ 0.3     |
| F3             | 6.3 $\pm$ 0.1     |
| F6             | 6.4 $\pm$ 0.2     |
| F9             | 6.6 $\pm$ 0.1     |
| F10            | 6.5 $\pm$ 0.2     |
| F11            | 6.3 $\pm$ 0.3     |
| F12            | 6.5 $\pm$ 0.2     |

Table 6: The weight and thickness of MN patches (mean  $\pm$  SD) n = 3

| Formula number | Thickness (mm)  | Weight (mg)      |
|----------------|-----------------|------------------|
| F2             | 0.52 $\pm$ 0.02 | 457.5 $\pm$ 2.22 |
| F5             | 0.52 $\pm$ 0.01 | 451.0 $\pm$ 1.01 |
| F6             | 0.55 $\pm$ 0.04 | 447.2 $\pm$ 2.87 |
| F9             | 0.53 $\pm$ 0.02 | 452.3 $\pm$ 1.28 |
| F10            | 0.56 $\pm$ 0.03 | 463.3 $\pm$ 3.10 |
| F11            | 0.53 $\pm$ 0.01 | 457.5 $\pm$ 2.22 |
| F12            | 0.54 $\pm$ 0.02 | 452.3 $\pm$ 1.28 |

Table 7: Percent moisture absorb and loss of MN patches (mean  $\pm$  SD) n=3

| Formula number | PML             | PMA              |
|----------------|-----------------|------------------|
| F2             | 2.33 $\pm$ 0.12 | 6.57 $\pm$ 0.42  |
| F5             | 2.43 $\pm$ 0.23 | 12.57 $\pm$ 0.42 |
| F6             | 2.94 $\pm$ 0.12 | 6.43 $\pm$ 0.33  |
| F9             | 2.12 $\pm$ 0.12 | 11.57 $\pm$ 0.21 |
| F10            | 3.10 $\pm$ 0.22 | 8.03 $\pm$ 0.41  |
| F11            | 4.15 $\pm$ 0.32 | 9.80 $\pm$ 0.29  |
| F12            | 3.54 $\pm$ 0.24 | 8.43 $\pm$ 0.33  |

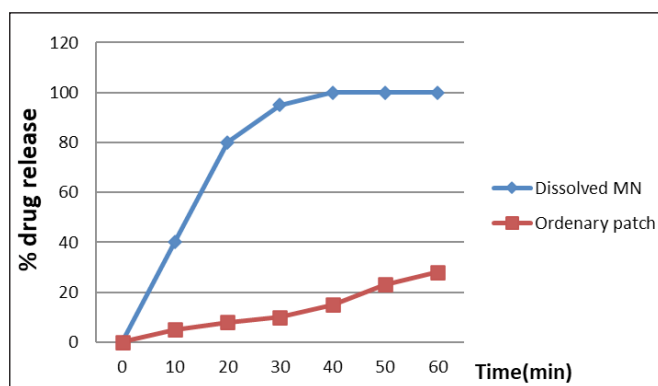


Figure 4: Percent of drug released from ordinary and dissolved MN

depicts MLX permeation profiles derived from the ordinary patch and MN patch and because of the MLX simple patched applied to undamaged skin had lower permeability than the other group (with MN patch). The permeated amounts of MLX in the ordinary patch group were the lowest among other groups (MN patch) at all-time points. Pretreatment with solid MNs opened up micropores in the skin, allowing MLX to diffuse from the outside into the skin. As a result, the MN patch showed rapid penetration, as seen by Figure 4. The needle matrix disintegrated quickly; the dissolving MNs injected MLX directly into the skin. Because there was no diffusion step from outside the skin into the skin, MLX was able to permeate the dissolving MNs even faster than the ordinary patch administered to the skin that was agreed with many earlier research<sup>50</sup> have shown that dissolving MNs can be an effective technique for increasing the penetration rate and delivery efficiency of an encapsulated medication.

## CONCLUSIONS

Because of its systemic absorption, oral MLX for the treatment of rheumatoid arthritis, osteoarthritis, and other joint conditions, could produce side effects. Transdermal MLX delivery could raise local medication concentrations, reduce administration frequency, and improve patient compliance. In this work, MLX-loaded MNs were created. The PVA17.5% matrix had great mechanical strength for penetrating the skin and was released soon after insertion. Micro molding techniques were used to make MLX MN patches. The desired level of medication content was discovered in all of the formulations. The right PVA ratio will give us the desired fraction force, quick disintegration, and an excellent permeability profile. Within 1-hour, the improved formula F6 (PVA17.5% and 10% PEG400) revealed 100% drug release.

## REFERENCES

- Amjadi M, Mostaghaci B, Sitti M. Recent advances in skin penetration enhancers for transdermal gene and drug delivery. *Curr Gene Ther*. 2017;17(2):139-146.
- Bala P, Jathar S, Kale S, Pal K. Transdermal drug delivery system (TDDS)-a multifaceted approach for drug delivery. *J Pharm Res*. 2014;8(12):1805-1835.
- Patel A V, Shah BN. Transdermal Drug Delivery System: A Review. *Pharma Sci Monit*. 2018;9(1).
- Aljuffali IA, Lin C-F, Fang J-Y. Skin ablation by physical techniques for enhancing dermal/transdermal drug delivery. *J Drug Deliv Sci Technol*. 2014;24(3):277-287.
- Parhi R, Suresh P, Mondal S, Mahesh Kumar P. Novel penetration enhancers for skin applications: a review. *Curr Drug Deliv*. 2012;9(2):219-230.
- Walters KA. *Dermatological and Transdermal Formulations*. Vol 119. CRC Press; 2002.
- Ternullo S, de Weerd L, Holsaeter AM, Flaten GE, Škalko-Basnet N. Going skin deep: A direct comparison of penetration potential of lipid-based nanovesicles on the isolated perfused human skin flap model. *Eur J Pharm Biopharm*. 2017;121:14-23.
- Godin B, Touitou E. Transdermal skin delivery: predictions for humans from in vivo, ex vivo and animal models. *Adv Drug Deliv Rev*. 2007;59(11):1152-1161.
- Prausnitz MR, Mitragotri S, Langer R. Current status and future potential of transdermal drug delivery. *Nat Rev Drug Discov*. 2004;3(2):115-124.
- Wang J-S, Hung Y-J, Lu Y-C, et al. Difference between observed and predicted glycated hemoglobin at baseline and treatment response to vildagliptin-based dual oral therapy in patients with type 2 diabetes. *Diabetes Res Clin Pract*. 2018;138:119-127.
- Shakya P, Madhav NVS, Shakya AK, Singh K. Palatal mucosa as a route for systemic drug delivery: A review. *J Control release*. 2011;151(1):2-9.
- Del Río-Sancho S, Serna-Jiménez CE, Sebastián-Morelló M, et al. Transdermal therapeutic systems for memantine delivery. Comparison of passive and iontophoretic transport. *Int J Pharm*. 2017;517(1-2):104-111.
- Hegde NR, Kaveri S V, Bayry J. Recent advances in the administration of vaccines for infectious diseases: microneedles as painless delivery devices for mass vaccination. *Drug Discov Today*. 2011;16(23-24):1061-1068.
- Lee H, Choi TK, Lee YB, et al. A graphene-based electrochemical device with thermoresponsive microneedles for diabetes monitoring and therapy. *Nat Nanotechnol*. 2016;11(6):566-572.
- Blagus T, Markelc B, Cemazar M, et al. In vivo real-time monitoring system of electroporation mediated control of transdermal and topical drug delivery. *J Control Release*. 2013;172(3):862-871.
- Gill HS, Prausnitz MR. Coated microneedles for transdermal delivery. *J Control release*. 2007;117(2):227-237.
- DeMuth PC, Su X, Samuel RE, Hammond PT, Irvine DJ. Nano-layered microneedles for transcutaneous delivery of polymer nanoparticles and plasmid DNA. *Adv Mater*. 2010;22(43):4851-4856.
- Gratieri T, Alberti I, Lapteva M, Kalia YN. Next generation intra- and transdermal therapeutic systems: using non- and minimally-invasive technologies to increase drug delivery into and across the skin. *Eur J Pharm Sci*. 2013;50(5):609-622.
- Ito Y, Hagiwara E, Saeki A, Sugioka N, Takada K. Feasibility of microneedles for percutaneous absorption of insulin. *Eur J Pharm Sci*. 2006;29(1):82-88.
- Donnelly RF, Singh TRR, Alkilani AZ, et al. Hydrogel-forming microneedle arrays exhibit antimicrobial properties: potential for enhanced patient safety. *Int J Pharm*. 2013;451(1-2):76-91.
- Mohammed NMH, El-Drieny E, Eldurssi IS, El-Agory M. Effect of meloxicam on hematological and kidney histopathological changes in male mice. *J Adv Med Med Res*. Published online 2017:1-8.
- Tripathi KD. *Essentials of Medical Pharmacology*. JP Medical Ltd; 2013.

23. Cheung K, Das DB. Microneedles for drug delivery: trends and progress. *Drug Deliv*. 2016;23(7):2338-2354.
24. Chen B, Wei J, Tay FEH, Wong YT, Iliescu C. Silicon microneedle array with biodegradable tips for transdermal drug delivery. *Microsyst Technol*. 2008;14(7):1015-1019.
25. Raza SN, Kar AH, Wani TU, Khan NA. Formulation and evaluation of mouth dissolving films of losartan potassium using 32 factorial design. *Int J Pharm Sci Res*. 2019;10(3):1402-1411.
26. Sadeq ZA, Rajab NA, Abd Alhammid SN, Zaki H. Preparation, in-vitro Evaluation, Mechanical Characterization, and Release Of Nebivolol Hydrochloride as A Transdermal Film using combined Eudragite-Polyvinyl Alcohol as Adhesive Film Forming Polymer. *J Pharm Sci Res*. 2019;11(3):1052-1055.
27. Rajab NA, Rassol AAA, Assaf SM, Sallam A-SA. Preparation and evaluation of fentanyl transdermal patches using lidocaine as a model drug and azelaic acid as a penetration enhancer. *Int J Pharm Pharm Sci*. 2014;6:615--620.
28. Alkhiro AR, Ghareeb MM. Formulation and Evaluation of lornoxicam as Dissolving Microneedle Patch. *Iraqi J Pharm Sci (P-ISSN 1683-3597, E-ISSN 2521-3512)*. 2020;29(1):184-194.
29. Chaisson D. Dissolution performance testing of transdermal systems. *Dissolution Technol*. 1995;2(1):7-11.
30. Ammar HO, Ghorab M, Mahmoud AA, Makram TS, Noshi SH. Topical liquid crystalline gel containing lornoxicam/cyclodextrin complex. *J Incl Phenom Macrocycl Chem*. 2012;73(1):161-175.
31. Soujanya C, Satya BL, Reddy ML, Manogna K, Prakash PR, Ramesh A. Formulation and in vitro & in vivo evaluation of transdermal patches of lornoxicam using natural permeation enhancers. *Int J Pharm Pharm Sci*. 2014;6(4):282-286.
32. Bharkatiya M, Nema RK, Bhatnagar M. Designing and characterization of drug free patches for transdermal application. *Int J Pharm Sci drug Res*. 2010;2(1):35-39.
33. Singh A, Bali A. Formulation and characterization of transdermal patches for controlled delivery of duloxetine hydrochloride. *J Anal Sci Technol*. 2016;7(1):1-13.
34. Kumar SS, Behury B, Sachinkumar P. Formulation and evaluation of transdermal patch of Stavudine. *Dhaka Univ J Pharm Sci*. 2013;12(1):63-69.
35. Musnina Waodes, Nisa M, Aprianti R, *et al*. Formulation and physical characterization of curcumin nanoparticle transdermal patch. *Int J Appl Pharm*. Published online 2019:217-221.
36. Kanabar VB, Patel VP, Doshi SM. Formulation and evaluation of transdermal patch of Cefdinir with various polymers. *Pharma Innov*. 2015;4(6, Part B):74.
37. Rajab NA, Sadeq ZA. Studying The Effect of Changing Plasticizer on The Formulation of Mucoadhesive Buccal Patches Of Captopril. Published online 2016.
38. Lee I-C, He J-S, Tsai M-T, Lin K-C. Fabrication of a novel partially dissolving polymer microneedle patch for transdermal drug delivery. *J Mater Chem B*. 2015;3(2):276-285.
39. Gwak HS, Oh IS, Chun IK. Transdermal delivery of ondansetron hydrochloride: effects of vehicles and penetration enhancers. *Drug Dev Ind Pharm*. 2004;30(2):187-194.
40. Baccaro S, Pajewski LA, Scoccia G, Volpe R, Rosiak JM. Mechanical properties of polyvinylpyrrolidone (PVP) hydrogels undergoing radiation. *Nucl Instruments Methods Phys Res Sect B Beam Interact with Mater Atoms*. 1995;105(1-4):100-102.
41. Shim WS, Hwang YM, Park SG, Lee CK, Kang NG. Role of polyvinylpyrrolidone in dissolving microneedle for efficient transdermal drug delivery: in vitro and clinical studies. *Bull Korean Chem Soc*. 2018;39(6):789-793.
42. Ahmad Z, Khan MI, Siddique MI, *et al*. Fabrication and characterization of thiolated chitosan microneedle patch for transdermal delivery of tacrolimus. *Aaps Pharmscitech*. 2020;21(2):1-12.
43. Wang C, Ye Y, Hochu GM, Sadeghifar H, Gu Z. Enhanced cancer immunotherapy by microneedle patch-assisted delivery of anti-PD1 antibody. *Nano Lett*. 2016;16(4):2334-2340.
44. Permana AD, McCrudden MTC, Donnelly RF. Enhanced intradermal delivery of nanosuspensions of antifilaria drugs using dissolving microneedles: a proof of concept study. *Pharmaceutics*. 2019;11(7):346.
45. Mofidfar M, Prausnitz MR. Design, structure, material strength and release profile of dissolvable microneedle patches. In: *Proceedings of the Society for Biomaterials 2018 Annual Meeting and Exposition*; 2018.
46. Arora P, Mukherjee B. Design, development, physicochemical, and in vitro and *in vivo* evaluation of transdermal patches containing diclofenac diethylammonium salt. *J Pharm Sci*. 2002;91(9):2076-2089.
47. Sonjoy M, Thimmasetty J, Ratan GN, Kilarimath BH. Formulation and evaluation of carvedilol transdermal patches. *Int Res J Pharm*. 2011;2(1):237-248.
48. Kameyama Y, Matsuhama M, Mizumaru C, Saito R, Ando T, Miyazaki S. Comparative Study of Pharmacopoeias in Japan, Europe, and the United States: Toward the Further Convergence of International Pharmacopoeial Standards. *Chem Pharm Bull*. 2019;67(12):1301-1313.
49. Zainab AS, Nawal AR. Studying the effect of different variables on the formulation of mucoadhesive buccal patches of captopril. *Int J Appl Pharm*. 2017;9:16-21.
50. Yang H, Kang G, Jang M, *et al*. Development of Lidocaine-Loaded Dissolving Microneedle for Rapid and Efficient Local Anesthesia. *Pharmaceutics*. 2020;12(11):1067.